Snow Depth and Ice Thickness Measurements From the Beaufort and Chukchi Seas Collected During the AMSR-Ice03 Campaign

Matthew Sturm, James A. Maslanik, Donald K. Perovich, Julienne C. Stroeve, Jackie Richter-Menge, Thorsten Markus, *Member, IEEE*, Jon Holmgren, John F. Heinrichs, *Member, IEEE*, and Ken Tape

***Abstract*—In March 2003, a field validation campaign was conducted on the sea ice near Barrow, AK. The goal of this campaign was to produce an extensive dataset of sea ice thickness and snow properties (depth and stratigraphy) against which remote sensing products collected by aircraft and satellite could be compared. Chief among these were products from the Polarimetric Scanning Radiometer (PSR) flown aboard a NASA P-3B aircraft and the Aqua Advanced Microwave Scanning Radiometer for the Earth Observing System (AMSR-E). The data were collected in four field areas: three on the coastal sea ice near Barrow, AK, and the fourth out on the open ice pack 175 km northeast of Barrow. The snow depth ranged from 9.4–20.8 cm in coastal areas ($n = 9881$ for three areas) with the thinnest snow on ice that had formed late in the winter. Out in the main pack ice, the snow was 20.6 cm deep ($n = 1906$). The ice in all four areas ranged from 138–219 cm thick ($n = 1952$), with the lower value again where the ice had formed late in the winter. Snow layer and grain characteristics observed in 118 snow pits indicated that 44% of observed snow layers were depth hoar; 46% were wind slab. Snow and ice measurements were keyed to photomosaics produced from low-altitude vertical aerial photographs. Using these, and a distinctive three-way relationship between ice roughness, snow surface characteristics, and snow depth, strip maps of snow depth, each about 2 km wide, were produced bracketing the traverse lines. These maps contain an unprecedented level of snow depth detail against which to compare remote sensing products. The maps are used in other papers in this special issue to examine the retrieval of snow properties from the PSR and AMSR-E sensors.**

***Index Terms*—Cryosphere, field validation, sea ice, snow.**

I. Introduction

ARCTIC SEA ice is covered by snow most of the year, the brief exceptions being when the ice first forms and during the short Arctic summer after the snow has melted. The properties and depth of the snow are strongly related to the age and character of the ice [1]–[4]. On first-year ice, the older the ice, the more time snow has to accumulate, and the deeper it gets. Postdepositional snow metamorphism is usually more advanced on older first-year floes, so these have a greater prevalence of both hard winds slabs and large depth hoar crystals than younger floes. Deeper snow also tends to be found on rougher ice, but in this case, ice roughness, not age, determines the snow depth. Rough ice traps wind-blown snow more effectively than smooth ice. In principle, knowing the age of the ice and its deformational history, along with the snow history, we should be able to predict the snow depth distribution. In practice, the heterogeneity of the real ice environment makes this type of prediction difficult.

There are several reasons why we need to know the snow distribution. One reason is that snow is an excellent thermal insulator [5]–[7] and can reduce the rate at which the ice thickens thermodynamically [8], [9]. The depth of the snow, its metamorphic state, and its areal distribution, all impact heat flow through the ice and therefore the rate of ice growth. Areas where the snow is thin release a disproportionate amount of oceanic heat during the winter in contrast to areas where it is thick [4]. The snow is also an important source of freshwater to the Arctic Ocean. Melting snow forms freshwater ponds on the ice that affect the surface energy exchange [10], [11]. These drain into the ocean to produce freshwater lenses that have thermal, biological, and oceanographic importance. Snow depth and density are also important when using altimetry to estimate ice thickness. Snow drifted in the lee of ice ridges provides denning material for seals, which are the main food resource for polar bears [12].

A final reason for wanting to know about the snow, and the chief motivation for this paper, is that it complicates the interpretation of sea ice remote sensing and, in particular, the retrieval of sea ice properties from passive microwave data. Snow and ice have similar dielectric properties at passive microwave frequencies [13], [14]: the observed signal comes from the combined contribution of both materials when snow overlies sea ice. The challenge is to take the combined signal and from it determine the properties of each component. As the Arctic climate continues to warm [15]–[18] it is crucial that we will be able to accurately track the changes occurring in the Arctic Ocean [17], [19], [20], and the only practical way to do this is by the effective use of remote sensing.

To that end, we conducted a field campaign in March 2003 on the sea ice near and offshore of Barrow, AK [21]. The general

Manuscript received November 14, 2005; revised April 18, 2006.

M. Sturm and J. Holmgren are with the U.S. Army Cold Regions Research and Engineering Laboratory–Alaska, Fort Wainwright, AK 99703 USA (e-mail: msturm@crrel.usace.army.mil).

J. A. Maslanik is with the Colorado Center for Astrodynamics Research, University of Colorado, Boulder, CO 80262 USA.

D. K. Perovich and J. Richter-Menge are with the U.S. Army Cold Regions Research and Engineering Laboratory, Hanover, NH 03755 USA.

J. C. Stroeve is with the National Snow and Ice Data Center, Cooperative Institute for Research in Environmental Sciences, University of Colorado, Boulder, CO 80309 USA (e-mail: stroeve@kryos.colorado.edu).

T. Markus is with the Laboratory for Hydrosperic Processes, NASA Goddard Space Flight Center, Greenbelt, MD 20771 USA (e-mail: Thorsten.Markus@nasa.gov).

J. F. Heinrichs is with the Department of Geosciences, Fort Hays State University, Hays, KS 67601 USA (e-mail: jheinric@fhsu.edu).

K. Tape is with the Geophysical Institute, University of Alaska–Fairbanks, Fairbanks, AK 99775 USA.

Digital Object Identifier 10.1109/TGRS.2006.878236

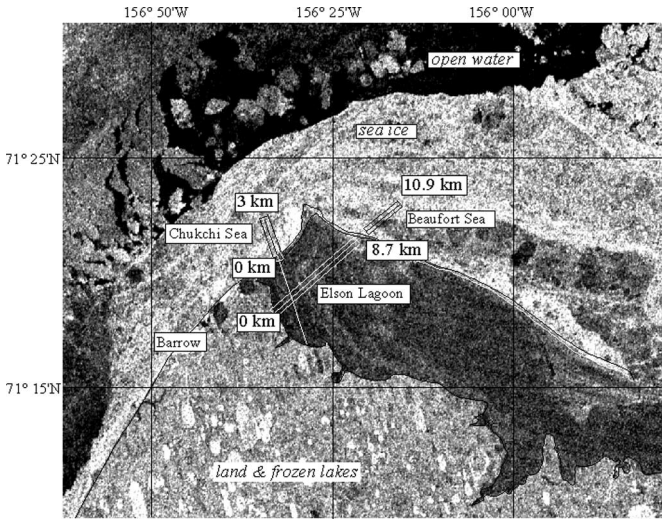

Fig. 1. Barrow field area showing the traverse lines and the three subareas (Chukchi, Elson, and Beaufort) where measurements were made. Box outlines indicate where snow depths were mapped using aerial photographs. The kilometer marks indicate distance along the traverse line and are referred to in the text. The base map is a SAR image from March 1999, a time when ice conditions were similar to those during the study.

goal of the campaign was to improve snow and ice retrieval algorithms from passive microwave remote sensing. The particular goal was to improve on our ability to interpret products from the Advanced Microwave Scanning Radiometer for the Earth Observing System (EOS AMSR-E). The campaign had field and aircraft components, the former of which is reported on here. The field program consisted of a detailed set of snow and ice measurements along a series of transects across the shore-fast ice near Barrow and out on the main pack ice 175 km north of Barrow. Each field transect became the center-line of an aircraft flight line along which detailed comparisons have been made between the Polarimetric Scanning Radiometer (PSR) results and the measured properties. These are reported in other papers in this issue [22], [23].

II. Field Area

We collected measurements from two main areas. The Navy Ice Camp was located at 72 °N, 55′ N, 147° 34′ W, about 175 km North East of Barrow, AK, in the main pack ice of the Arctic Ocean. The area was a mix of first-year (FYI) and multiyear ice (MYI) floes with moderate ridging. The second area was on the shore-fast ice in the vicinity of Barrow, AK (71° 19′ N, 156° 41′ W). It had three subareas–the Chukchi Sea, Beaufort Sea, and Elson Lagoon (Fig. 1)–each of which had distinctive snow drift characteristics that had their origin in different ice conditions (Fig. 2). Elson Lagoon, protected by barrier islands, had very smooth FYI and large rolling snowdrifts. The near-shore ice on the Chukchi Sea was also smooth FYI but with a few low (< 0.5 m) pressure ridges. It was thinner and younger than the Elson ice. The FYI of the Beaufort Sea had undergone moderate (< 1 m) to heavy ridging (> 5 m) and new ice formation in leads. Consequently, this subarea with quite rough surface topography had a wide range of snow conditions that included drifts in excess of 1.5 m deep as well as wind-scoured areas where there was little or no snow on the ice. As discussed later, snow and ice conditions in the Beaufort subarea proved to be similar to those at the Navy Ice Camp.

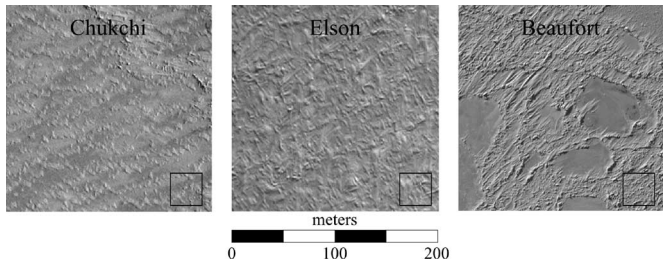

Fig. 2. Snow surface conditions in the three study subareas. Each image is 200 by 200 m. The open boxes are 30 by 30 m and represent the footprint size for the aircraft PSR sensor.

TABLE I
Measurement Methods Used During AMSR-Ice03 Field Campaign

Measurement	Method and Accuracy
Snow depth	Self-recording depth probe; ±0.3 cm
Snow density	100 cm^3 steel cutter weighed on digital balance; ±0.05 g/cm^3
Snow water equivalent	Federal snow coring tube; contents weighed; ±0.5 cm water equivalent.
Snow-ice interface temperature	Digital thermistor probe inserted through the snow pack to refusal at the ice surface; ±0.3°C
Snow stratigraphy	Pit wall brushed and measured with ruler relative to ice surface
Snow grain size	Stereo-microscope comparison to a gridded card; estimates of average long and short dimensions of grains as well as grain type. A few samples were sieved [25, 26].
Ice thickness (drilling)	Ice auger; ±1 cm
Ice thickness (EM-31)	Electro-magnetic device [24]; ±3 cm
Ice salinity	Salinity meter; ±0.5 ppt
Ice temperature	Digital thermistor probe; ±0.3°C

In each area, we surveyed in traverse lines that were then marked with posts drilled into the ice. The posts were labeled with the distance from the start of the line (usually the nearest shore); snow and ice measurements were keyed to these kilometer markers (Fig. 1). Large (5 m) black tetrahedra (constructed from two-by-fours and black roadbed fabric) marked the start and end of each line. Ground measurements at the Navy Ice Camp were made along a main line 4.47 km long (orientation N14 °E), and five cross lines each 0.1 km long.

Measurements in the Barrow area were made between March 4, 2003 and March 19, 2003. Aerial photographs (in digital form) were taken from a Cessna 185 aircraft on March 7 and March 11. A NASA P-3B aircraft overflew the Barrow field area on March 13 and again on March 19. During the field campaign, there was almost no new snow accumulation and relatively limited redistribution of snow by the wind, hence measurements taken throughout the campaign represent a "stable" snow cover.

III. Field Methods

We measured snow depth, density, water equivalent, stratigraphy, and grain size using the methods listed in Table I. We measured sea ice thickness using an electromagnetic method (an EM-31, see [24] and http://www.geonics.com/em31.html). The EM-31 was calibrated by drilling through the ice and comparing the measured ice thickness with the computed value from the EM-31, then adjusting the formula until the latter agreed with the former. Cores of the ice were taken using a corer

and analyzed for salinity. We measured ice roughness using a laser level and range pole along a tape that had been laid out on the ice. Sea level datum for these profiles was established by drilling a hole in the ice. During the overflights by the NASA P-3B aircraft, field personnel measured the snow–ice interface temperature and the temperature 0.1 m below the ice surface in as many places as possible. This was done in as short a time as possible (about 3 h) to avoid diurnal variations in temperature. The snow–ice interface temperature was measured by forcing a thermistor probe (accurate to ± 0.3 °C) down through the snow to ice surface, allowing the probe equilibrate for a minute, and then reading the temperature on a digital readout. For the ice temperature, we used a cordless drill to drill a hole to a depth of 10 cm in the ice and then placed the probe in the hole. This depth was chosen because it is an easy depth to drill to, and because the 10 cm temperature and the ice surface temperature provide good values from which the bulk ice temperature can be computed. The weather during the campaign was recorded at three portable meteorological stations, while air and ice temperatures were recorded at nine locations throughout the field area. In addition, Barrow is a first order National Weather Station reporting temperature, wind speed, and direction, precipitation, and sky conditions (http://weather.noaa.gov/weather/current/PABR.html).

Snow depth was measured every 0.5 m along 100-m lines at 15 separate stations. It was also measured at ∼4-m spacing along traverse lines that ranged from 2–5 km in length, for a cumulative total of more than 18.4 km of probing. Ice thickness was measured electromagnetically (using the EM-31) along the same lines at approximately the same spacing. It was checked and calibrated by drilling through the ice at 25 locations. Snow pits ($n = 118$) were equispaced along these lines to capture the essential snow stratigraphy across the study subareas.

Vertical aerial photographs bracketing the transect lines were taken from a Cessna 185 using a Nikon digital camera. The aircraft flew at 1200 m, producing images with a ground resolution of about 0.7 m. Particularly during the March 7 flight, the lighting conditions were superb (low-angle direct sun) producing photographs with unusually fine detail that highlighted the surface roughness. Uncontrolled (i.e., we did not create a network of survey points within the coverage area) photomosaics were prepared from these photographs using Panavue software (http://www.panavue.com/index.htm). Using identifiable ice features, the ground-based traverse lines, as well as the location of the kilometer-makers along the lines, were placed on these mosaics and ultimately transferred to snow maps prepared from the photographs. Photographs were not available for the Navy Ice Camp line.

IV. Results

The ice near Barrow was FYI. At the Navy Ice Camp, there were a few MYI floes interspersed with mostly FYI. The FYI in Elson Lagoon, protected by barrier islands, underwent little deformation, though as described in other papers in this issue [23], [27] some localized roughness was present. The Chukchi ice was moderately deformed, while the ice of the Beaufort Sea near Barrow and out at the Navy Ice Camp was moderately to heavily deformed. The snow cover everywhere was relatively thin (< 0.3 m) except near pressure ridges and rafted ice blocks, where drifts in excess of 1 m could be found. As has been found in other areas [4], [28] the snow pack consisted primarily of wind-blown slabs (drift snow) and depth hoar, the latter a coarse-grained type of snow produced when snow is subjected to a strong temperature gradient and metamorphoses.

Despite the difference in location, the ice in the Beaufort Sea subarea had similar snow cover characteristics as the Navy Ice Camp [Fig. 3(a)]. It also had a similar distribution of ice thickness [Fig. 3(b)], and a similar mean thickness (though ice thinner than 140 cm was missing in the near-shore location). A reasonable explanation for the similarity in snow cover was that the ice in both areas had undergone similar amounts of deformation, had similar surface roughness characteristics, and therefore trapped similar snow packs. The high coefficients of variation (CV, defined as the ratio of the standard deviation to the mean) for snow depth and ice thickness indicate that rough ice trapped a deep, heterogeneous snow cover in both locations (Table II).

In the Elson and Chukchi subareas, the ice was less rough and the snow was thinner [Fig. 3(a) and (b)]. The ice on Elson Lagoon formed about the same time as the ice on the Beaufort Sea, but as noted above, it underwent almost no deformation relative to the off-shore ice. This accounts for the lack of a thick ice tail in the histogram shown in Fig. 3(b). The low CV value (Table II) indicates that Elson ice had relatively smooth upper and lower surfaces. The smooth nature of the ice allowed the winter wind to drift the snow cover with relative ease, creating large regular drifts (barchans and whalebacks [29]). These were bigger and more regular than those that formed on the rougher ice in the Beaufort subarea and at the Navy Ice Camp. Large drifts like these are also found on the smooth ice of the large tundra lakes in the Barrow region [30].

In the Chukchi subarea, the shore-fast sea ice initially formed at the same time as in the other areas, but this ice was swept out to sea during a storm in December. The ice on which we made our measurements formed after this storm and was distinctly thinner than in the other subareas. Once the new ice had formed, it remained in place with relatively little deformation (in the area where we made our measurements). This gave rise to the narrow, peaked ice histogram shown Fig. 3(b). We suspect that the snow drifts on the Chukchi ice might eventually have grown as large as those on Elson Lagoon, since the ice was almost as smooth, but the amount of snow available for drifting was limited by the age of the ice. Consequently, the Chukchi subarea had the thinnest snow pack of all of the field areas. As shown in Fig. 3(a), the snow depth distribution histogram was even tighter than that of Elson Lagoon [Fig. 3(b)].

Based on results from 118 snow pits, the snow pack in all of the areas consisted primarily of layers of depth hoar overlain by wind slabs. There were also fine-grained and thin icy layers in a few locations. As might be expected given the younger ice in the Chukchi Sea subarea, the snow pack there had fewer layers than otherwise (Table III). At the Navy Ice Camp, the wind slab fraction was slightly higher than in the other areas, perhaps a result of stronger winds out in the open ice pack. At all of the areas, depth hoar layers typically consisted of grains with long dimensions ranging from 2–10 mm, and short dimensions ranging from 0.1–0.3 mm (i.e., thin, platelike grains). The depth hoar grain size distribution was highly mixed, consisting of both large and small grains. In contrast, the wind slab layers

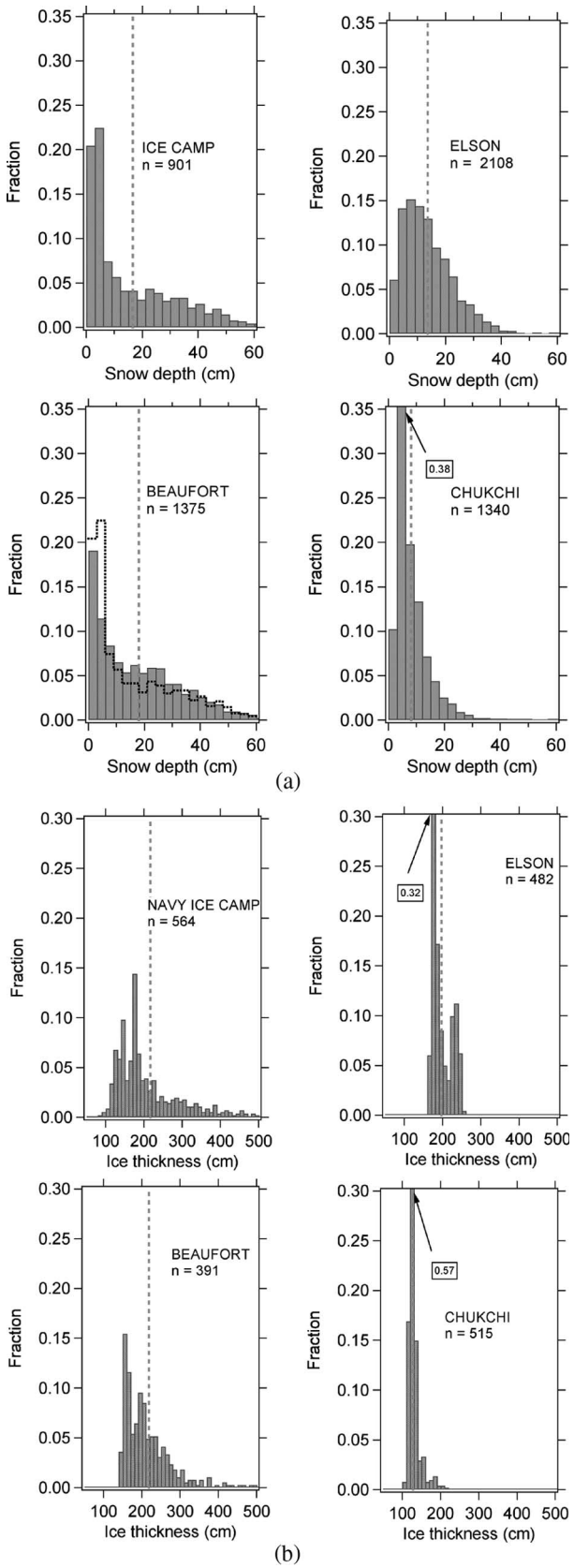

Fig. 3. (a) Probability distribution functions of snow depth for the four subareas. The vertical dashed lines indicate the mean values. A histogram for the Navy Ice Camp (black dashed line) has been superimposed on the histogram for the Beaufort Sea to emphasize the similarity in the two PDFs. (b) PDFs of ice thickness for the four subareas. The vertical dashed line indicates the mean value.

TABLE II
SNOW DEPTH AND ICE THICKNESS STATISTICS
(CV = coefficient of variation = Std. Dev./Mean Depth)

	n	Mean Depth (cm)	Std. Dev. (cm)	CV
SNOW DEPTH				
Navy Ice Camp	1906	20.6	18.8	0.913
Beaufort Sea	2593	20.8	20.6	0.99
Elson Lagoon	4319	12.7	8.5	0.669
Chukchi Sea	2969	9.4	8.1	0.86
ICE THICKNESS				
Navy Ice Camp	564	217	106	0.488
Beaufort Sea	391	219	90	0.411
Elson Lagoon	482	197	26	0.132
Chukchi Sea	515	138	14	0.103

TABLE III
AVERAGE TEXTURAL MAKE-UP OF THE SNOW PACK FOR THE SUBAREAS

	Navy Ice Camp	Beaufort	Elson	Chukchi
Number of Layers:	4	5	4	2
Mean layer thickness (cm)	7.6	6.3	3.9	3.9
Bulk density (g/cm3)	0.36	0.28	0.36	0.32
Hoar Fraction	0.36	0.48	0.51	0.44
Slab Fraction	0.58	0.35	0.40	0.51
Other Fraction	0.06	0.17	0.09	0.05
Number of Snowpits	25	23	35	35

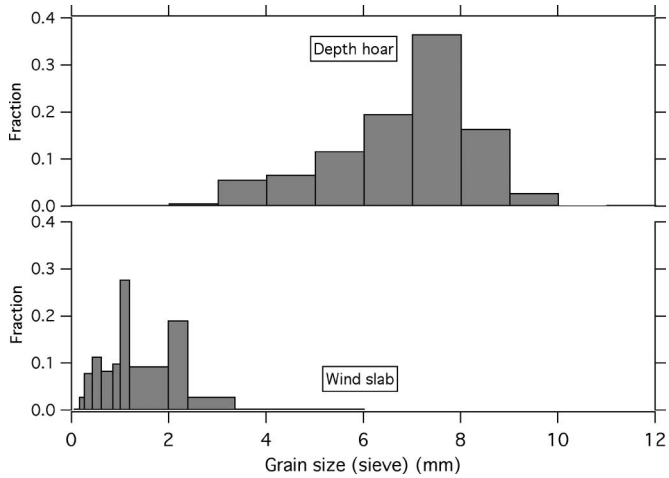

Fig. 4. Typical grain size distributions for depth hoar and wind slab snow, the most common snow in the study areas.

were well sorted and composed of equant grains that ranged in diameter from 0.1–0.9 mm. Results of sieve analysis (Fig. 4, see [25] and [26] for methodology) show the grain size distributions for these two predominant types of snow.

In all locations, the snow layers were discontinuous, pinching out where they intersected ice obstructions, thickening in the lee of ice blocks and ridges. As a result, the number of layers, and the nature of the layers, varied markedly over relatively short (< 1 m) lateral distances. A typical cross section of the

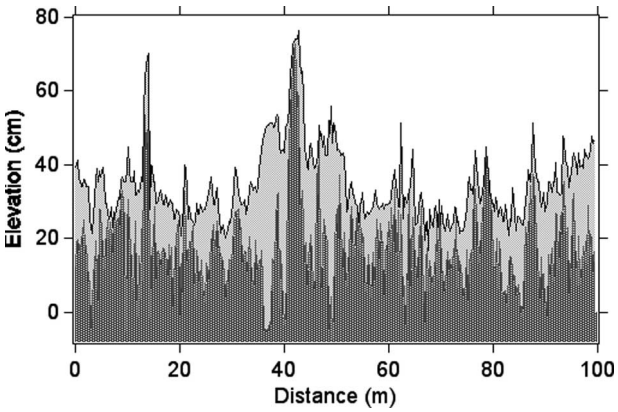

Fig. 5. Typical cross section of snow (light gray) and ice (dark gray), in this case from the Beaufort subarea (vertical exaggeration: 50X). In a few locations, the ice surface is below the water surface and the snow may have been wet in those areas.

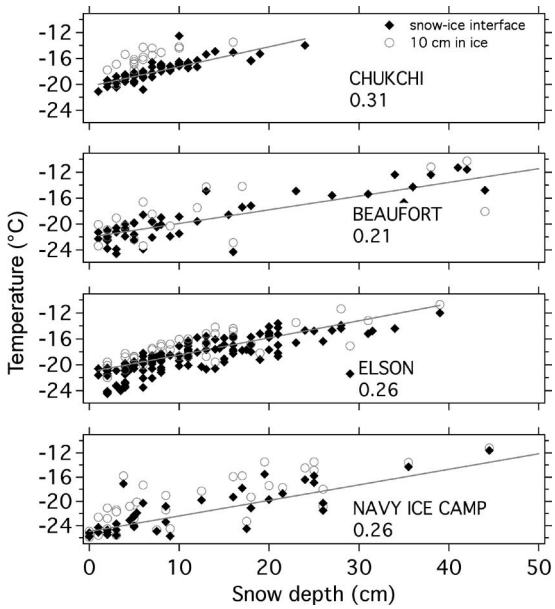

Fig. 6. Snow–ice interface temperatures, and ice temperatures at 10-cm depth measured during the day of the PSR overflight. The values below the site names indicate the slope of the line fit to the data, or the increase in temperature (degrees Celcius per centimeter) with increasing snow depth.

snow pack and ice surface, in this case from the Beaufort Sea subarea, is shown in Fig. 5. From a semivariogram analysis [4], [31], [32] the characteristic length scale of the surface roughness of the ice in the example shown was about 2 m, while the length scale of the snow roughness was about 20 m. The drifting snow has "smoothed" the ice surface by producing longer wavelength features, though these have about the same amplitude as that of the underlying ice hummocks. This type of smoothing was typical wherever we encountered rough ice in the study. A similar result has been reported for both Arctic [4] and Antarctic snow and sea ice [28].

Ice and snow–ice interface temperatures were made during the overflight of the NASA P-3B aircraft. Fortuitously, the overflights occurred during a period of generally stable, low air temperature. Daytime highs hovered near -20 °C, and nighttime lows dropped consistently to -28 °C to -30 °C. These diurnal fluctuations were damped out by the snow pack and ice, producing snow–ice interface and ice temperatures that were temporally stable since they were subjected to essentially a "steady-state" driving temperature. Linear regressions of measured temperatures versus snow depth by subareas have slopes that vary over a narrow range (0.21 °C to 0.31 °C/cm snow depth: see values in each panel of Fig. 6). The congruence of these regression lines suggests that in all areas the lower part of the snow pack and the upper part of the ice were functioning something like an isothermal block during the period of the study, and that the snow pack had much the same thermal impact (per unit thickness) in all areas. There are some differences, however. In the Chukchi and Elson subareas, ice temperatures at 10 cm depth tended to be slightly higher than the interface temperature. In the Chukchi subarea, the ice was thinner than otherwise, and conductive heating from the ocean water could account for this bias. In the Elson subarea, where the ice was nearly as thick in the Beaufort areas, thin snow cannot be invoked, and the reason for the bias is not known. As discussed by Markus *et al.* [22], snow and ice temperatures affect brightness temperatures and therefore appear in the retrieval algorithms for passive microwave remote sensing of sea ice. The snow–ice interface temperature is also a standard product from the AMSR-E satellite. The temperature data were collected in order to validate the retrieval algorithm for that product.

We found a strong relationship between ice roughness, snow surface characteristics (i.e., snow drift patterns: see Fig. 2) and snow depth. In the Beaufort Sea and Navy Ice Camp subareas, near pressure ridges and in rubble fields, the snow pack was deep with large variations in depth (Figs. 7 and 8). On the intervening smooth floes, the snow was thin (or absent) and relatively uniform. Snow from these smooth floes had been blown into adjacent rough ice areas where it had been trapped. This pattern of alternating deep variable snow and thin uniform snow was particularly striking for the Beaufort subarea, where ocean currents and wind had sheared the ice into an mélange of rounded floes surrounded by ridges and rubble fields (see [23] for additional details). On the smoother ice of Elson Lagoon and the Chukchi Sea, the snow depth was more independent of ice surface conditions, controlled instead by the processes that create snow ripples, dunes, and barchans. While the genesis of these features is not well understood, particularly with respect to what determines their geometry [29], the size and regular spacing of the dunes was constrained: they tended to range from 10–50 m in length and 20–50 cm in height.

Superimposed on the snow depth variations caused by ice ridges, rubble, and dune formation were depth variations at a larger scale ($>$ 200 m). We speculate that these were synoptic in origin. In all the subareas except Elson Lagoon these larger scale patterns were masked by other, larger depth variations (i.e., drifts in the lee of ridges). For Elson Lagoon, where the ice was smooth and the traverse line long ($>$ 8 km), the variations have been plotted in Fig. 9. Depth data were collected at approximately 4-m intervals ($n = 2108$) along the traverse line. Using 200 passes of a binomial filter [33] we have produced from the original data a smoothed depth record that resolves variations over distances of about 100 m and greater. We have divided the smooth curve into 6 segments for each of which we have computed the local mean. Different choices in smoothing resulted in only slightly different segments, with

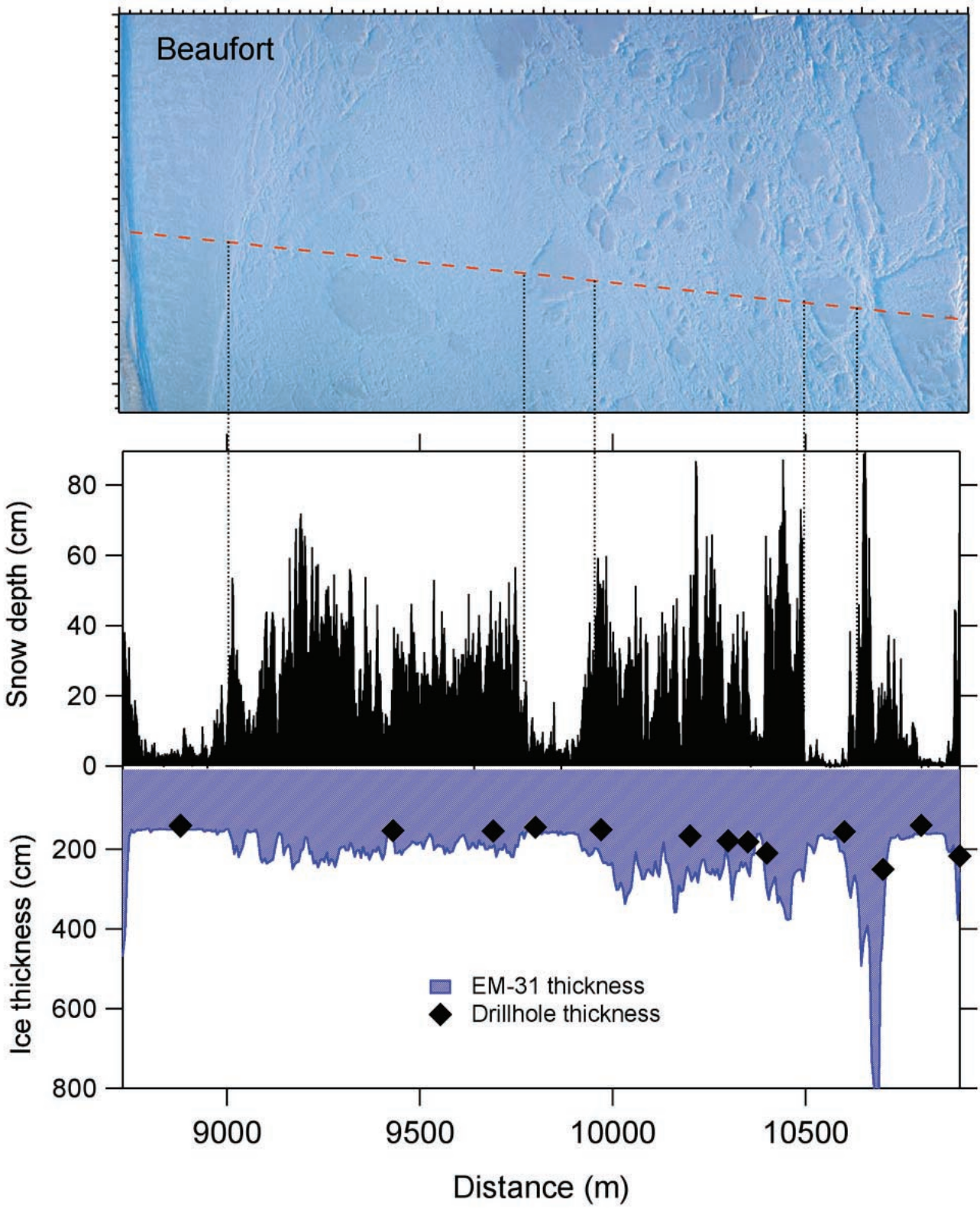

Fig. 7. (Middle panel) Snow depth and (lower panel) ice thickness on the main Beaufort line correlated with (top panel) the air photographs mosaic.

the salient features illustrated in Fig. 9 in large measure preserved. The segments suggest variations in snow depth at scales ranging from 200–2500 m. The source of the variation is uncertain, but could be related to local variations in wind and snowfall.

V. Mapping Snow Depth Using Snow–Ice Relationships

The distinct three-way relationship between ice roughness, snowdrift characteristics, and snow depth can be used to

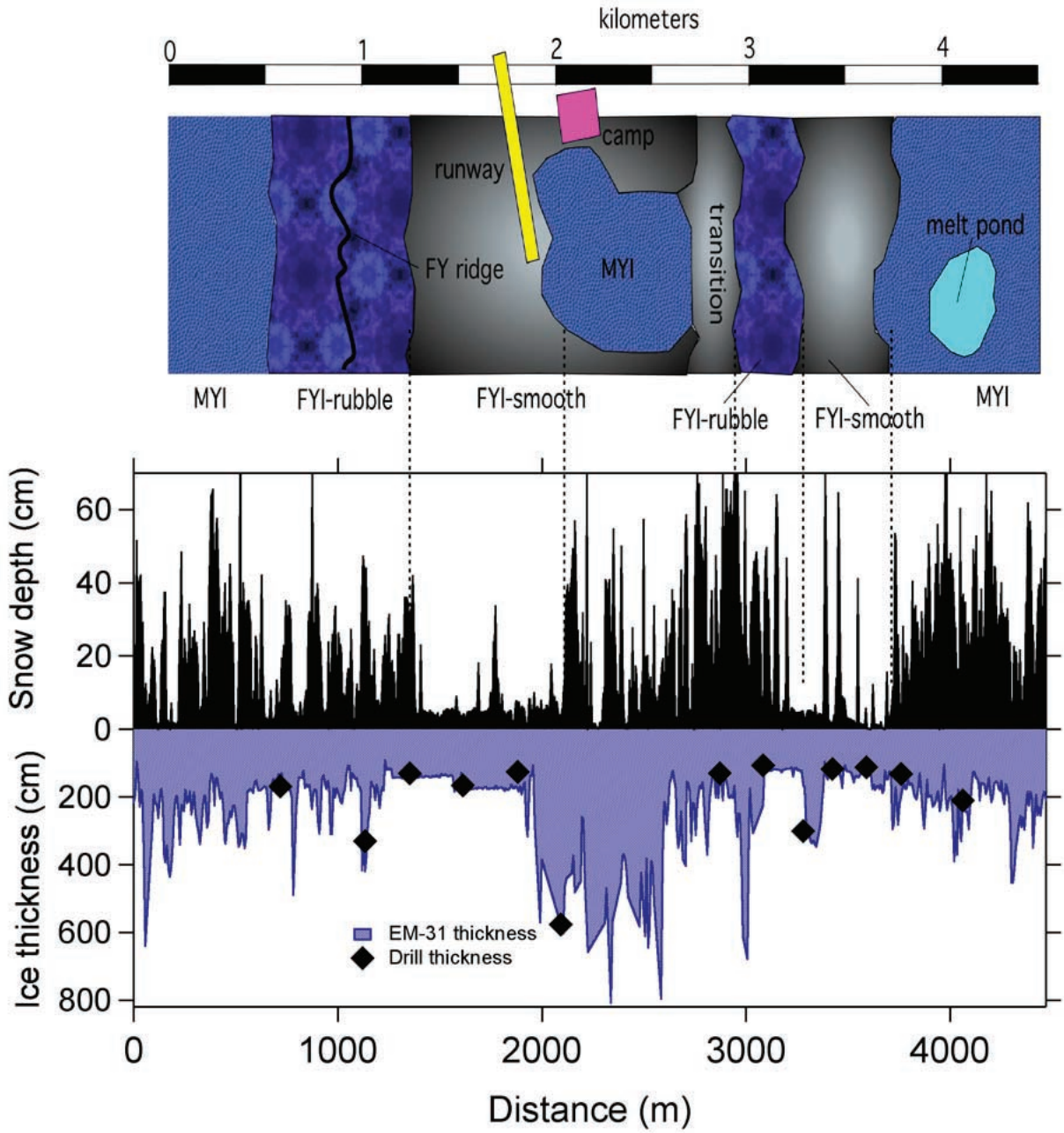

Fig. 8. (Middle panel) Snow depth and (lower panel) ice thickness on the main Navy Ice Camp line correlated with (top panel) an ice map sketched in the field by a trained observer.

produce maps of snow depth for the area covered by the aerial photographs. This snow depth mapping is particularly useful for extrapolating snow depth from linear transects to areal domains (e.g., [23]), thereby making it easier to compare remote sensing products to field data. To facilitate the mapping, we defined three classes of ice: 1) smooth; 2) moderately deformed; and 3) heavily deformed (ridges and rubble fields). These were easily identified in the field and were recorded in field notes. We found that the ice classes could be either FYI or MYI. Each of these ice classes had a "characteristic look" on air photographs arising from the unique snowdrifts patterns (Figs. 2, 7, and 8) imparted to the snow by the ice roughness. By inspection, we noted that the smooth ice had a snow pack less than 10 cm deep, rough ice had a snow pack deeper than 25 cm, and moderately deformed ice had a snow cover between 10 to 25 cm deep (Table IV). The class divisions were the same at the Navy Ice Camp and the Beaufort subareas. Using 10 and 25 cm as critical snow depths, we divided data from the traverse lines into sectors with common depth characteristics, computing for each a set of statistics (Fig. 10 and Table IV). Where applicable, we augmented the main traverse depth record with data from 100-m profile lines taken nearby.

Using image analysis software (NIH ImageJ: http://rsb.info.nih.gov/ij/features.html) and the aerial photomosaics, we were able to differentiate the three types of ice based on snow drift patterns. To do this, we used an iterative, empirical approach following the processing steps listed in Table V. The processing steps were established for areas where there were measured snow depth data. By trial and error, threshold values of 25 and 55 were identified. Using these values, the steps listed in

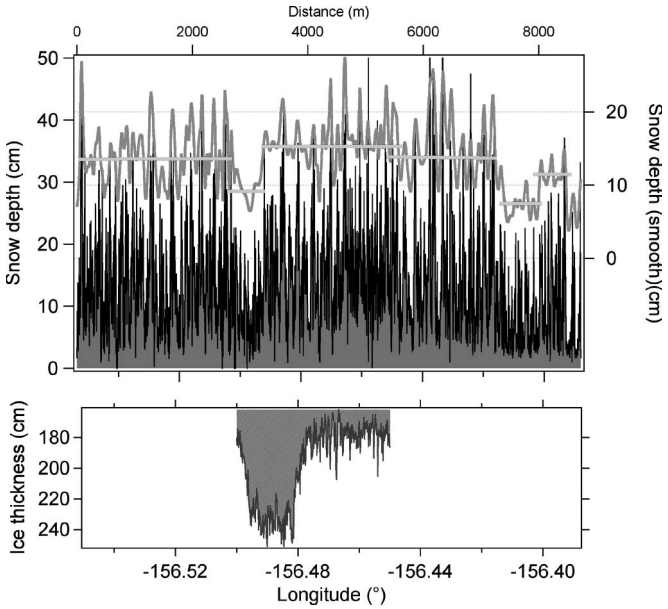

Fig. 9. (Left) Measured and (right) smoothed snow depth along the main Elson Lagoon measurement line. The six segments discussed in the text are shown as horizontal lines.

Table V were then applied to areas where measurements had not been made. The result is a set of maps [Fig. 11(a)–(c)] of snow depth. Using the results of Fig. 6, snow–ice interface temperatures could be mapped as well. The same algorithm developed for the Beaufort subarea was applied without adjustment to the Elson and Chukchi subareas (photographs were not available for the Navy Ice Camp). A comparison of measured and mapped snow depths for the Chukchi and Elson subareas indicate accurate mapping for the Chukchi (where $> 90\%$ of the snow was less than 10 cm deep and mapped as such).

Results were less favorable for the Elson subarea, where the steps listed in Table V overestimated the depth [Fig. 11(c), compare bottom panel to top panel]. One problem encountered for the Elson subarea was that the aerial photographs had a radial gradient in brightness (due to the digital camera lens characteristics) that confounded the image processing, producing deeper snow in the middle of each photograph, thinner snow on the edges. To improve the results, for the Elson subarea, we altered the threshold values (Table V, step 4, a value of 35; step 5, a value of 65), and used a narrower strip from the center of the photographs where the variable lighting was not as bad. The result [Fig. 11(c)] matched the field data better, but still overestimated the depth.

VI. Discussion

A fundamental issue when trying to validate remote sensing products is that field data invariably consist of a series of point measurements, while remote sensing data cover areas or swaths. In this paper, we tried to overcome that problem by: 1) taking extensive closely spaced data and 2) utilizing natural relationships between snow accumulation and ice roughness to map snow depth in places where it had not been measured. The large number of depth measurements (13 212), the unusually long length of our measurement lines (18.4 km), and quality of our aerial photograph, may have been unprecedented for an ice validation campaign. They have allowed us to use the mapping approach listed in Table V and as a result produce more detailed and extensive areal snow depth data against which to compare the remote sensing than has been available previously. Elsewhere, a direct comparison of the snow depth maps and PSR data are presented [23] and discussed.

At the center of the field validation issue are the dual problems of: 1) coregistration of aerial and ground data and 2) differences in footprint size. Even the "homogeneous" snow and ice of Elson Lagoon had snow depth variations at scales ranging from a few tens of meters (Fig. 2: drifts and dunes) to up to 2500 m [Fig. 9: variations due to gradients in precipitation and wind]. In this subarea, if there was an undetected offset between the sensor footprint and the field data, it could produce an apparent mismatch between PSR-derived ice and snow properties and those that were measured. In the rougher ice of the Navy Ice Camp and the Beaufort Sea, the coregistration problem is even more severe. There, an offset of 30 m (the size of the PSR footprint [22]) might result in a shift in snow depth equal to the full range of depths observed during the study (i.e., from bare ice to a deep drift).

We see these two issues as particularly crucial when remotely sensing an environment that is as spatially heterogeneous as the arctic sea ice and its snow cover. A 30-m footprint (open square) has been superimposed on each panel in Fig. 2 to highlight how the sensor footprint size compares to the grain of the snow–ice environment. The possibility of an inadvertent misregistration of field and remote data suggest a correlation of map patterns needs to be used when comparing the two sets of information. Our use of transect data in combination with our extensive ice reconnaissance, photograph mosaics, and other imagery helps alleviate problems associated with registration by allowing us to extrapolate across space scales, but the issue remains a critical one for data analysis. For sea-ice studies, the problem is further exacerbated by the fact that the ice pack moves and evolves over time. For studies conducted over shore-fast ice, such as near Barrow, the temporal ice change problem is greatly reduced and the resulting comparisons allow spatial registration and footprint matching to be explored without the confusion of temporal change as well.

VII. Conclusion

An extensive set of snow and ice data were collected during the AMSR-E validation campaign at four areas near and off-shore of Barrow, AK. These areas ranged from relatively smooth undeformed ice with thin snow cover to pressure ridges with deep and highly variable snow cover. The snow consisted mainly of wind slabs and depth hoar, typically in equal measure. snow–ice interface and near-surface ice temperatures were a strong function of snow depth. Snow depth could be related to ice roughness, and could be identified in aerial photographs by distinctive drift patterns. This led to a simple image-processing algorithm that allowed us to create snow depth maps covering areas of several square kilometers. These are used otherwise in this volume to validate the PSR sensor.

The results reinforce a well-known fact: the snow and ice environment of the Arctic sea ice is extremely heterogeneous. This heterogeneity extends from ice thickness and snow depth to physical temperature, grain size, snow water equivalent, and

TABLE IV
DEPTH STATISTICS FOR SECTORS OF THE BEAUFORT AND NAVY ICE CAMP SNOW LINES; THE RANGE IS A MEASURE OF THE SNOW STRUCTURE LENGTH SCALE. SECTOR VALUES LIKE 2.90 km REFER TO DATA TAKEN FROM A 100-m TRANSECT LOCATED AT THAT KILOMETER MARKER

NAVY ICE CAMP

Ice Class	Sector	Mean (cm)	Std. dev. (cm)	Max. (cm)	Min. (cm)	Range (m)	Type of Ice	n
	2.90 km	44	19	85	3	7	MYI & FYI, large rubble	201
HEAVILY	E	28	22	87	0	80	FYI, rubble	120
DEFORMED	G	26	18	117	0	100	MYI, rubble	157
	4.47 km	24	13	69	1	12	MYI, widely spaced rubble	201
	0.83 km	22	17	62	0	23	FYI, rubbly	201
MODERATELY	0.14 km	21	16	69	0	14	FYI low rubble, flat	201
DEFORMED	A	18	17	80	0	55	MYI, low rubble	130
	B	16	13	74	0	55	FYI, low rubble	150
	D	15	17	72	0	120	FYI, low rubble	96
	2.11 km	10	14	51	0	14	MYI, smooth	201
SMOOTH	F	7	12	70	0	26	FYI, smooth	108
	C	6	4	34	0	47	FYI, smooth	146

BEAUFORT

Ice Class	Sector	Mean (cm)	Std. dev. (cm)	Max. (cm)	Min. (cm)	Range (m)	Type of Ice	n
	10.9km	49	31.1	122	3	9	FYI, ridge	201
HEAVILY	I	37.4	19.3	89	0	5	FYI, ridge	61
DEFORMED	C	34.8	14.2	72	3	8	FYI, rubble & ridge	123
	8.92km	34.3	15.6	72	5	2	FYI, rubble & ridge	201
	G	24.1	15.8	88	0	30	FYI, rubble	239
	E	23.2	11.1	57	0	14	FYI, rubble	218
MODERATELY	K	19.1	17.4	90	0	29	FYI, rubble	83
DEFORMED	B	16.9	11.5	53	2	8	FYI, rubble	112
	H	15.9	10.9	46	0	14	FYI, mod. Smooth	71
	D	15.5	10.8	52	2	15	FYI, mod. Smooth	64
	F	4.4	3.9	19	0	4	FYI, smooth	86
	9.97km	4.3	3.5	21	0	3	FYI, smooth	201
SMOOTH	L	3.1	4.2	10	0	6	FYI, smooth	92
	A	2.98	1.93	11	0	2	FYI, smooth	119
	10.6km	2	2.9	19	0	8	FYI, smooth	201
	J	1.3	1.9	8	0	4	FYI, smooth	73

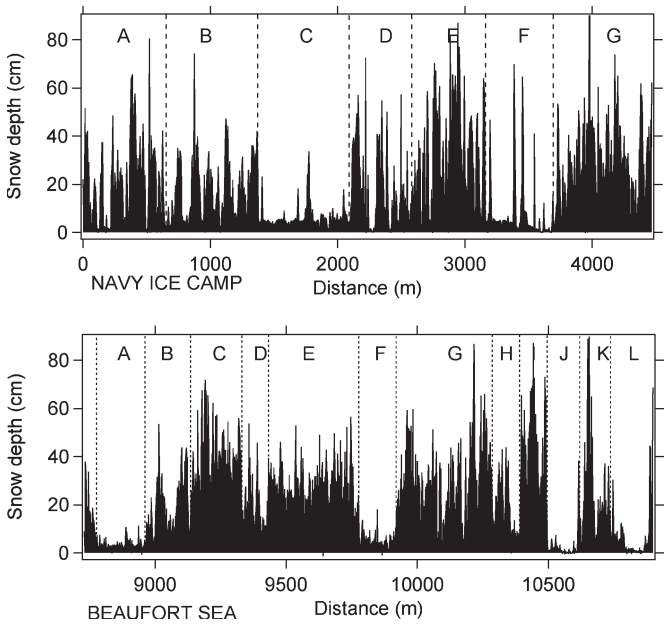

Fig. 10. Sector analysis for the Beaufort and Navy Ice Camp main snow depth lines. The sector letters are keyed to Table IV. The locations of these additional data are indicated by their names; i.e., Sector 2.90 km is data from a 100-m long line located near the 2.90 km mark on the main line.

TABLE V
IMAGE PROCESSING STEPS

Step	Description
1	Separate image into RGB colors; discard R and G layers
2	Pass a variance filter (radius 5 pixels) over the B image.
3	Smooth the resulting image using a Gaussian filter (radius 27 pixels)
4	Assign pixels below 25 to the smooth ice class; produce a smooth ice class binary image (smooth, not smooth)
5	Assign pixels between 25 and 55 to the moderately deformed ice class; produce a moderate ice class binary image (moderate, not moderate)
6	Assign pixels greater than 55 to the rough ice class; produce a rough ice class binary image (rough, not rough)
7	Produce a ternary color map of the 3 ice types by combining layers from steps 4-6
8	Interpret ice roughness map in terms of snow depth using Table 4

roughness. In many cases, the spatial scale of the variability is less than 10 m, and only for a few attributes does the scale extend to hundreds of meters or more. One impact from this heterogeneity is that all pixels, satellite or aircraft, are "mixed" (i.e., consist of a combination of different surfaces). The fact that meaningful retrievals can be made from the remote sensing data imply that (fortunately) key geophysical properties tend to aggregate around mean values, but exactly how various ice/snow elements are amalgamated remains unclear.

One surprising finding from the field data was that the snow conditions in the Beaufort Sea shore-fast ice zone, just a few kilometers off of the land, were similar to the conditions at the Navy Ice Camp, 175 km off-shore. This similarity existed, despite the fact that the near-shore Beaufort ice was FYI, while the off-shore Beaufort ice was mixed MYI and FYI. We attribute this overall similarity to the fact that roughness, not age or type of ice, was the controlling variable, with the degree of deformation the critical factor. Thus, the near- and off-shore Beaufort ice had similar roughness; this led to similar snow-holding capacity and similar temperature conditions. These similarities between the Barrow-area shore-fast ice and the pack

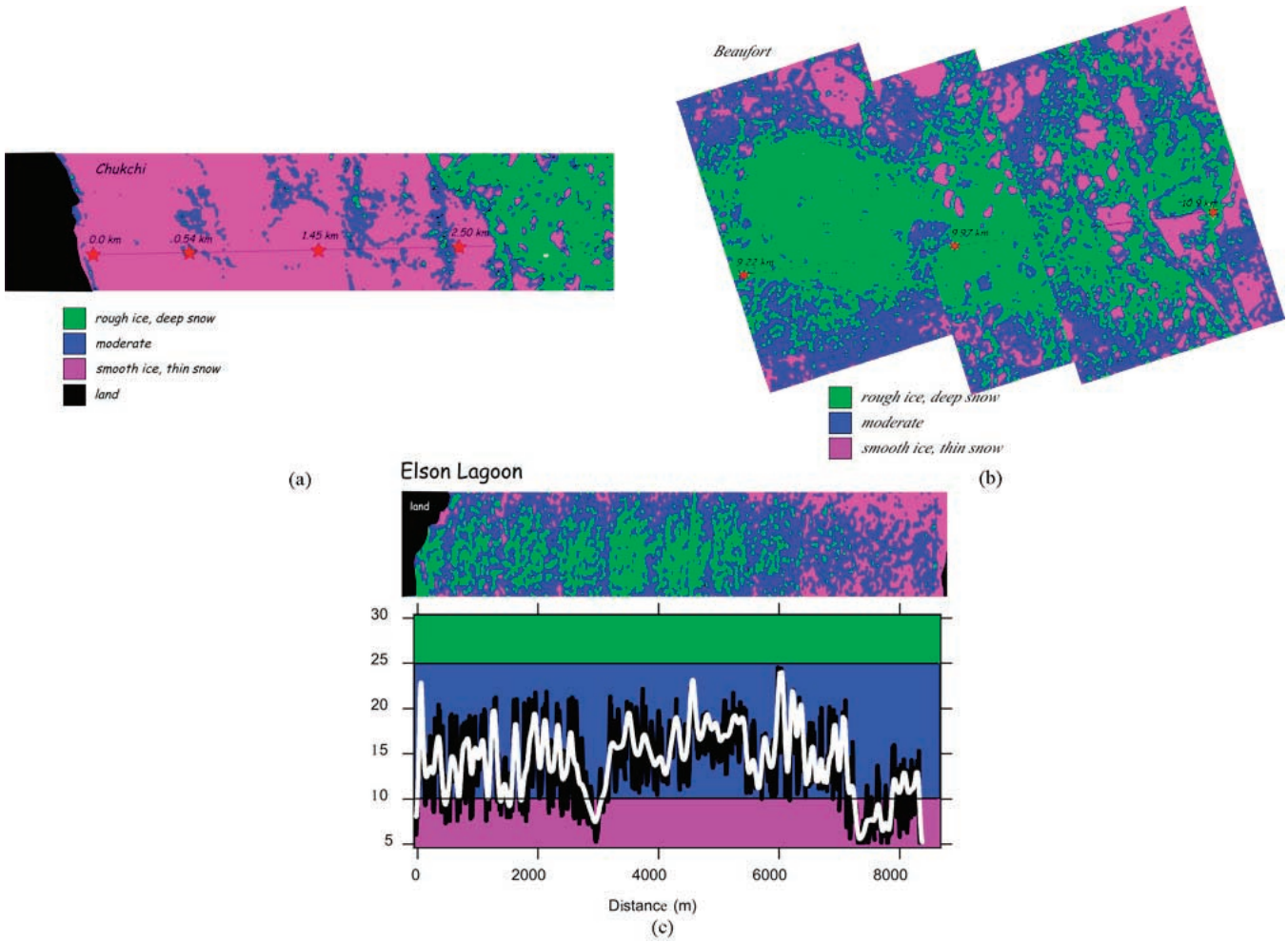

Fig. 11. (a) Snow depth map for the Chukchi Sea subarea produced from aerial photographs, as described in the text. (b) Snow depth map for the Beaufort Sea subarea produced from aerial photographs, as described in the text. (c) (Top) A snow depth map for the Elson Lagoon subarea produced from aerial photographs, as described in the text. (Bottom) Snow depth (black) and snow depth smoothed (white) along the traverse line, showing how the maps tend to overestimate the depth in this subarea.

ice at the Ice Camp lessen concerns about the representativeness of the shore-fast ice data to overall sea ice conditions.

ACKNOWLEDGMENT

The authors would like to thank the Barrow Arctic Science Consortium for providing logistics for the field campaign. They would also like to thank G. Sheehan and R. Glenn. W. Matumeak provided field advice from his long experience on the sea ice. T. Douglas, W. Simpson, and others enthusiastically participated in the fieldwork. D. Cavalieri provided encouragement and support for the entire concept of an in-depth field campaign. Three anonymous reviewers provided comments that led to substantial improvements in the paper.

REFERENCES

[1] A. M. Hanson, "The snow cover of sea ice during the Arctic Ice Dynamics joint experiment, 1975–1976," *Arct. Alp. Res.*, vol. 12, no. 2, pp. 215–226, 1980.

[2] M. Sturm, K. Morris, and R. Massom, "The winter snow cover of the West Antarctic pack ice: Its spatial and temporal variability," in *Antarctic Sea Ice Physical Processes, Interactions and Variability*, M. O. Jeffries, Ed. Washington, DC: Amer. Geophys. Union, 1998, pp. 1–18.

[3] J. Iacozza and D. G. Barber, "An examination of the distribution of snow on sea-ice," *Atmos.—Ocean*, vol. 37, no. 1, pp. 21–51, 1999.

[4] M. Sturm, J. Holmgren, and D. K. Perovich, "Winter snow cover on the sea ice of the Arctic Ocean at the surface heat budget of the Arctic Ocean (SHEBA): Temporal evolution and spatial variability," *J. Geophys. Res.*, vol. 107, no. C10, p. 8047, 2002, DOI:10.1029/2000JC000400.

[5] M. Mellor, *Properties of Snow*. Hanover, NH: U.S. Army Cold Regions Res. Eng. Lab., 1964.

[6] T. S. Ledley, "Snow on sea ice: Competing effects in shaping climate," *J. Geophys. Res.*, vol. 96, no. D9, pp. 17 195–17 208, 1991.

[7] M. Sturm, J. Holmgren, M. König, and K. Morris, "The thermal conductivity of seasonal snow," *J. Glaciol.*, vol. 43, no. 143, pp. 26–41, 1997.

[8] N. Untersteiner, "On the mass and heat budget of Arctic sea ice," *Arch. Meteorol. Geophys. Bioklimatol.*, vol. A, no. 12, pp. 151–182, 1961.

[9] G. A. Maykut and N. Untersteiner, "Some results from a time-dependent thermodynamic model of sea ice," *J. Geophys. Res.*, vol. 76, no. 6, pp. 1550–1575, 1971.

[10] H. Eicken, H. R. Krouse, D. Kadko, and D. K. Perovich, "Tracer studies of pathways and rates of meltwater transport through Arctic summer sea ice," *J. Geophys. Res.*, vol. 107, no. C10, pp. SHE22-1–SHE22-20, 2002, DOI:10.1029/2000JC000583.

[11] H. Eicken, T. C. Grenfell, D. K. Perovich, J. A. Richter-Menge, and K. Frey, "Hydraulic controls of summer Arctic pack ice albedo," *J. Geophys. Res.*, vol. 109, no. C08007, 2004, DOI:10.1029/2003JC001989.

[12] N. Rozell, "Jeopardy: Alaska's polar bears face threat of a changing climate," *Alaska Mag.*, pp. 49–56, Oct. 2004.

[13] M. Hallikainen and D. Winebrener, "The physical basis for sea ice remote sensing," in *Microw. Remote Sens. Sea Ice—Monograph 68*. Washington, DC: Amer. Geophys. Union, 1992, pp. 29–46.

[14] D. Eppler *et al.*, "Passive microwave signatures of sea ice," in *Microw. Remote Sens. Sea Ice—Monograph 68*, F. Carsey, Ed. Washington, DC: Amer. Geophys. Union, 1992, pp. 47–71.
[15] W. L. Chapman and J. E. Walsh, "Recent variations of sea ice and air temperature in high latitudes," *Bull. Amer. Meteorol. Soc.*, vol. 74, no. 1, pp. 33–47, Jan. 1993.
[16] M. C. Serreze, J. E. Walsh, F. S. Chapin, III, T. Osterkamp, M. Dyurgerov, V. Romanovsky, W. C. Oechel, J. Morison, T. Zhang, and R. G. Barry, "Observational evidence of recent climate change in the northern high-latitude environment," *Clim. Change*, vol. 46, no. 1/2, pp. 159–207, 2000.
[17] J. C. Comiso and C. L. Parkinson, "Satellite-observed changes in the Arctic," *Phys. Today*, vol. 57, no. 8, pp. 38–44, Aug. 2004.
[18] L. D. Hinzman *et al.*, "Evidence and implications of recent climate change in northern Alaska and other Arctic regions," *Clim. Change*, vol. 72, no. 3, pp. 251–298, Oct. 2005, DOI:10.1007/s10584-005-5352-2.
[19] M. C. Serreze *et al.*, "A record minimum Arctic sea ice extent and area in 2002," *Geophys. Res. Lett.*, vol. 30, no. 3, 1110, 2003, DOI:10.1029/2002GLO16406.
[20] W. Meier, J. Stroeve, F. Fetterer, and K. Knowles, "Reductions in Arctic sea ice cover no longer limited to summer," *EOS*, vol. 86, no. 36, pp. 326–327, Sep. 2005.
[21] D. J. Cavalieri, T. Markus, J. A. Maslanik, M. Sturm, and E. Lobl, "March 2003 EOS Aqua AMSR-E Arctic sea ice field campaign," *IEEE Trans. Geosci. Remote Sens.*, vol. 44, no. 11, pp. 3003–3008, Nov. 2006.
[22] T. Markus, D. J. Cavalieri, A. J. Gasiewski, M. Klein, J. A. Maslanik, D. C. Powell, B. B. Stankov, J. C. Stroeve, and M. Sturm, "Microwave signatures of snow on sea ice: Observations," *IEEE Trans. Geosci. Remote Sens.*, vol. 44, no. 11, pp. 3081–3090, Nov. 2006.
[23] J. A. Maslanik *et al.*, "Spatial variabliity of Barrow-area shore-fast sea ice and its relationship to passive microwave emissivity," *IEEE Trans. Geosci. Remote Sens.*, vol. 44, no. 11, pp. 3021–3031, Nov. 2006.
[24] A. Kovacs, D. Diemand, and J. J. Bayer, "Electromagnetic Induction Sounding of Sea Ice Thickness," Cold Regions Res. Eng. Lab., Hanover, NH, CRREL Tech. Rep. 96-6, 1996.
[25] M. Sturm, The role of thermal convection in heat and mass transport in the subarctic snow cover. Hanover, NH: U.S. Army Cold Regions Res. Eng. Lab., 1991.
[26] M. Sturm and C. S. Benson, "Vapor transport, grain growth and depth hoar development in the subarctic snow," *J. Glaciol.*, vol. 43, no. 143, pp. 42–59, 1997.
[27] U. C. Herzfeld, J. A. Maslanik, and M. Sturm, "Geostatistical characterization of snow-depth structures on sea ice near point Barrow, Alaska—A contribution to the AMSR-Ice03 field validation campaign," *IEEE Trans. Geosci. Remote Sens.*, vol. 44, no. 11, pp. 3038–3056, Nov. 2006.
[28] R. A. Massom, H. Eiken, C. Haas, M. O. Jeffries, M. R. Drinkwater, M. Sturm, A. P. Worby, X. Wu, V. I. Lytle, S. Ushio, K. Morris, P. A. Reid, S. G. Warren, and I. Allison, "Snow on Antarctic sea ice," *Rev. Geophys.*, vol. 39, no. 3, pp. 413–445, 2001.
[29] G. A. Doumani, "Surface structures in snow," in *Proc. Int. Conf. Low Temperature Sci.: I. Phys. Snow and Ice*, Sapporo, Japan, 1966, pp. 1119–1136.
[30] M. Sturm and G. Liston, "The snow cover on lakes of the Arctic coastal plain of Alaska, U.S.A.," *J. Glaciol.*, vol. 49, no. 166, pp. 370–380, 2003.
[31] I. Clark, "The semivariogram," in *Geostatistics*. New York: McGraw-Hill, 1980, pp. 17–40.
[32] E. H. Isaaks and R. M. Srivastava, *An Introduction to Applied Geostatistics*. New York: Oxford Univ. Press, 1989.
[33] P. Marchand and L. Marmet, "Binomial smoothing filter: A way to avoid some pitfalls of least-squares polynomial smoothing," *Rev. Sci. Instrum.*, vol. 54, no. 8, pp. 1034–1041, 1983.

Matthew Sturm received the M.S. and Ph.D. degrees in geophysics from the University of Alaska, Fairbanks, AK, in 1984 and 1989, respectively.

He is currently a Research Scientist with the U.S. Army Cold Regions Research and Engineering Laboratory-Alaska, Ft. Wainwright, AK. He has led over 15 Arctic expeditions. His research interests include Arctic climate change, snow on land, and snow on sea ice.

Dr. Sturm is a member of the American Geophysical Union, the International Glaciological Society, and the Arctic Institute of North America.

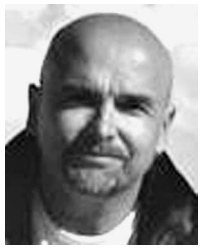

James A. Maslanik received the B.S. degree in forest science and the M.S. degree in environmental pollution control from the Pennsylvania State University, University Park, PA, in 1980 and 1978, respectively, and the Ph.D. degree in geography from the University of Colorado, Boulder, in 1984.

He is a Research Professor with the Department of Aerospace Engineering Sciences, University of Colorado. His research interests include the interactions of sea ice with atmosphere and ocean, remote sensing and field investigations of sea-ice properties, effects of climate change on Arctic coastal communities, and development and deployment of unpiloted aerial vehicles for polar research.

Donald K. Perovich received the M.S. and Ph.D. degrees in geophysics from the University of Washington, Seattle, in 1979 and 1983, respectively.

He is currently a Research Geophysicist with the Snow and Ice Branch, U.S. Army Cold Regions Research and Engineering Laboratory, Hanover, NH. He has conducted wide-ranging studies on sea ice, with special focus on optical properties and radiative transfer in sea ice. He was the Chief Scientist for the SHEBA Project, an experiment where a ship was frozen into the Arctic pack and allowed to drift for a year.

Dr. Perovich is a member of the American Geophysical Union, the International Glaciological Society, the American Meteorological Society, and the Electromagnetics Academy.

Julienne C. Stroeve received the B.S. and M.S. degrees in aerospace engineering and the Ph.D. degree in geography from the University of Colorado, Boulder, in 1989, 1991, and 1996, respectively, where she focused on surface energy balance studies of the Greenland ice sheet using satellite imagery.

Since 1996, she has been with the National Snow and Ice Data Center, Cooperative Institute for Research in Environmental Sciences, University of Colorado, Boulder, as a Research Scientist, specializing in remote sensing of snow and ice. She has extensive experience in remote sensing of the polar regions using satellite imagery that spans the optical to the microwave spectral region. She has participated in several field campaigns in Greenland and the Arctic for the purpose of validation of various geophysical parameters retrieved from spacecraft such as sea ice concentration, surface temperature, and surface reflectivity. Additional research projects include monitoring the rapid decline in ice cover in the Arctic and increased melt of the Greenland ice sheet. At NSIDC, she is responsible for the sea ice products derived from satellite passive microwave data, which includes aiding in the design of Web pages providing general sea ice information and data sets regarding the state of sea ice that may be useful to a broad audience.

Dr. Stroeve is a member of the IEEE Geoscience and Remote Sensing Society, the American Geophysical Union, and the Association of American Geographers.

Jackie Richter-Menge received the M.C.E. degree from the University of Delaware, Newark, in 1981.

She is currently a Research Civil Engineer with the Snow and Ice Branch, U.S. Army Cold Regions Research and Engineering Laboratory, Hanover, NH. Her research interests include sea-ice deformation and autonomous systems (buoys) for monitoring sea ice.

Ms. Richter-Menge is a Professional Civil Engineer of the State of New Hampshire. She is a member of the American Geophysical Union and the International Glaciological Society.

Thorsten Markus (M'05) received the M.S. and Ph.D. degrees in physics from the University of Bremen, Bremen, Germany, in 1992 and 1995, respectively.

He is currently a Research Scientist with the NASA Goddard Space Flight Center (GSFC), Greenbelt, MD. From 1995 to 1996, he was a National Research Council Resident Research Associate with GSFC before joining NASA-UMBC Joint Center for Earth Systems Technology, where he worked until 2002. His research interests include satellite microwave remote sensing of primarily ice and the utilization of satellite data to study oceanic and atmospheric processes.

Dr. Markus is a member of the American Geophysical Union.

Jon Holmgren received the B.S. degree in geology/geophysics from the University of Alaska–Fairbanks, Fairbanks, in 1987.

He is a Research Scientist with the U.S. Army Cold Regions Research and Engineering Laboratory-Alaska, Ft. Wainwright, where he develops instrumentation and apparatus for field and experimental projects, and operates a commercial machine shop. He has extensive experience in making measurements on sea ice.

John F. Heinrichs (M'06) received the B.S. and M.S. degrees in mathematics from the University of Wisconsin–Milwaukee (UWM), Milwaukee, in 1983 and 1985, respectively, and the Ph.D. degree in geography from the University of Colorado, Boulder, in 1996.

He was a Staff Scientist with the Hughes Aircraft Company from 1986 to 1992, a Research Assistant with the Cooperative Institute for Research in Environmental Sciences (CIRES), Boulder, from 1992 to 1996, and a Postdoctoral Researcher with CIRES from 1996 to 1998. Since 1998, he has been with the faculty of Fort Hays State University, Hays, KS, where he is currently an Associate Professor and the Chair of the Department of Geosciences.

Dr. Heinrichs is a member of the IEEE Geoscience and Remote Sensing Society, the American Geophysical Union, and the Association of American Geographers.

Ken Tape received the M.S. degree in geophysics from the University of Alaska–Fairbanks, Fairbanks, in 2006. He is currently working toward the Ph.D. degree in ecology at the University of Alaska-Fairbanks.

He has participated in numerous winter expeditions on the sea ice and tundra of northern Alaska.

Mr. Tape is a member of the American Geophysical Union.